

ARTIFICIAL NEURAL NETWORK PREDICTION PARAMETERS OF 10 % SF₆ – 90 % N₂ MIXTURE

FAISSEL BELOUCIF, AMAR BOUDEFEL, ASSIA GUERROUI, AHCENE LEMZADMI, ABDELKRIM MOUSSAOUI

Keywords: Sulfur hexafluoride; Gas mixture SF₆-N₂; Onset voltages; Corona discharges; Ionic mobility.

The present study outlines the application of artificial neural networks for the Prediction of corona discharge parameters in SF₆-N₂ gas mixture. The artificial neural network modeling is used to predict corona discharge temperature, ionic mobility, and onset voltages for different gas pressures with a mixture of 10 % SF₆ – 90 % N₂, and using experimental data obtained previously. The results of artificial neural networks' prediction of ionic mobility (μ) onset voltages (V_s) and temperature are found to be around $\pm 6\%$ for training as well as for testing and are significantly consistent with the experimental values.

1. INTRODUCTION

Sulfur hexafluoride is the electric power industry's preferred gas for electrical insulation and arc quenching capabilities. Generally, there are four major types of electrical equipment, which use SF₆ for insulation and/or interruption purposes: gas-insulated circuit breakers and current-interruption equipment, gas-insulated transmission lines, gas-insulated transformers, and gas-insulated substations. The properties of a gas that are necessary for its use in high voltage equipment are many and vary depending on the application of the gas and the equipment. Sulfur hexafluoride exhibits many properties that make it suitable for equipment utilized in electric power systems [1–3]. It is a strong electronegative (electron attaching) gas both at room temperature and at temperatures well above ambient, its dielectric strength is substantially greater than that of traditional dielectric gases and it has good arc-interruption properties. The breakdown voltage of SF₆ is nearly three times higher than air at atmospheric pressure; it has good heat transfer properties. SF₆ offers significant savings in land use, is aesthetically acceptable, has relatively low radio and audible noise emissions, and enables substations to be installed in populated areas close to the loads.

However, SF₆ has been found to be environmentally unacceptable and was listed among the seven greenhouse gases in the Kyoto Protocol [4]. It has a lifetime of 3200 years in the atmosphere and a global warming potential (GWP) on a 100-year horizon of 23 900 compared to CO₂ [5]. In fact, the concentration of SF₆ in the atmosphere increased by 20% from 2010 to 2015 [6].

The European regulation 517/2014 on fluorinated greenhouse gases [7] bans SF₆ in all applications except in high voltage technology. In the short term, the main option is to reduce the emission of SF₆. The potential candidate to substitute the SF₆ is the mixture of Sulphur hexafluoride and nitrogen (SF₆-N₂) with a small amount of SF₆. The mixture must satisfy all the requirements such as chemical, electrical, physical, and environmental properties [8,9].

Nitrogen (N₂) is the typical electron retarding gas in which, the fast electron can be slowed down and the electron energy can be reduced. This can be achieved by de-energizing electrons reaching higher energy and returning them to the lower energy range, where attachment by electronegative gas is most effective [10,11].

The overall cost of the system can be reduced depending on the cost of the buffer gas; furthermore, the use of dilute mixtures could provide a convenient solution to the pressing

problem of global warming associated with SF₆ leak.

The prediction of corona parameters in the gas mixture 10%SF₆-90%N₂, which is considered the favorite candidate to replace pure SF₆ is carried out using Artificial Neural Network (ANN) technique.

The ANNs can be used to predict the ionic mobility (μ), the onset voltages (V_s), and the temperature of the corona discharge. The main feature of neural networks is the establishment of complex relationships between data through a learning process [12,13]. This technique can be very attractive in the modeling of processes where traditional mathematical modeling is difficult or impossible.

Recent years have seen attempts by several authors to use various artificial neural networks (ANNs) based models [14–16]. The rationale here is that ANNs have the potential to provide a mechanism for dealing with multi-variant, often noisy, and possibly non-linear data sets, where an exact analytic model is either intractable or too time-consuming to develop. The basic procedure is to use a database of measurements to train an ANN structure and then evaluate the predictive capacity of the built model on previously unseen data.

2. SIMULATION METHOD

2.1. NEURAL NETWORKS MODEL

The proposed multi-layer neural network structure is shown in Fig. 1.

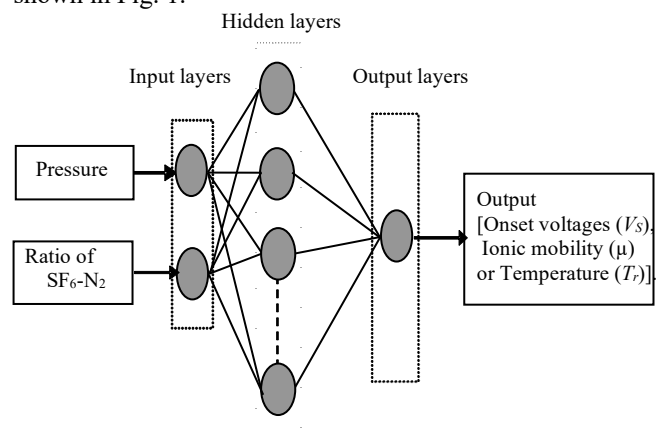


Fig. 1 – Architecture of different neurons into an artificial neural network (MLP).

It has two input layers, the gas pressure (P) and the ratio of N₂ in the gas mixture (r). The number of output layers is three, ionic mobility (μ), discharge rotational temperature (T_r), and onset voltage (V_s), as expressed in equations (1, 2,

and 3), W is the neural network weights.

$$\mu = NN(P, r, W). \quad (1)$$

$$T_r = NN(P, r, W). \quad (2)$$

$$V_s = NN(P, r, W). \quad (3)$$

The output is even that, onset voltages (V_s), ionic mobility (μ), or temperature (T_r), these values have the following expressions.

$$\mu = \sum_{j=1}^M W_{kj} \tanh \left[\sum_{i=1}^d W_{ji} x_i + b_j \right] + b_k. \quad (4)$$

$$T_r = \sum_{j=1}^M W_{kj} \tanh \left[\sum_{i=1}^d W_{ji} x_i + b_j \right] + b_k. \quad (5)$$

$$V_s = \sum_{j=1}^M W_{kj} \tanh \left[\sum_{i=1}^d W_{ji} x_i + b_j \right] + b_k. \quad (6)$$

where W_{ji} is the weight matrix of the first layer, W_{kj} is the weight matrix of the second layer, b_j is the bias vector of the first layer, b_k is the bias vector of the second layer, d is the number of input nodes and M is the number of hidden nodes.

The Hecht-Kolmogorov theorem [17,18], proposes that the number of neurons in the hidden layer must be greater than the double of the neurons in the input layer. The output layer has three neurons, such as the onset voltage, ionic mobility, and rotational temperature, corresponding to the input data. The training and testing of these neural networks were done using MATLAB® software.

To perform accurate learning, the output layer is normalized to have the same order of magnitude as the input layer.

2.2. LEARNING ALGORITHM

According to Fig. 2, the learning algorithm adjusts the weights in all connecting links and thresholds in the nodes so that the actual output $Y(t)$ and the target output $T(t)$ are minimized for all given training patterns.

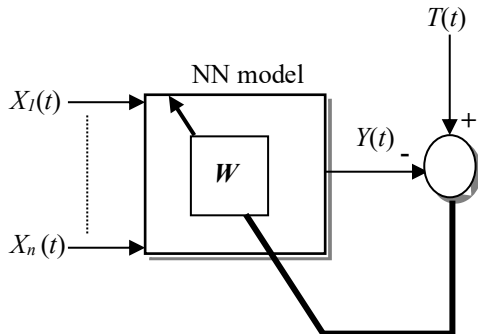


Fig. 2 – Learning Algorithm Scheme.

For the p^{th} training pattern ($p=1..P$), the learning algorithm is performed to minimize the energy function.

$$E_p = \frac{1}{2} \sum_i [T_i - Y_i(N)]^2. \quad (7)$$

Where, $Y_i(N)$ is the activation of i^{th} neuron in the output

layers N , T_i is the i^{th} desired output, and N is the number of layers. The application of Levenberg-Marquardt to neural network training is described in [19-21]. This algorithm appears to be the fastest method for training feed-forward neural networks. The weights are adjusted according to the iterative Levenberg-Marquardt updating:

$$W_{ij}^{(new)}(n) = W_{ij}^{(old)}(n) - [J^T J + aI]^{-1} J^T E_T. \quad (8)$$

where W_{ij} is the weight between i^{th} neuron of layer $n+1$ and j^{th} neuron of layer n , ($0 \leq n \leq N-1$), I is the identity matrix, J is the Jacobian matrix, which contains first derivatives of the network errors with respect to the weights and biases and E_T is a vector of all network errors.

The parameter a is adapted during the learning procedure. When the total error E_T goes below a predetermined threshold value E_{\min} , the learning algorithm is then stopped. Back-propagation is used to calculate the Jacobian J of the performance function E_p .

$$J = \frac{\partial E_p}{\partial W_{ij}(n)} = \delta_i(n) f'[u_i(n)] Y_j(n-1). \quad (9)$$

with $1 \leq i \leq L_{n+1}$ where:

$$\delta_i(n) = \sum_j \delta(n+1) \cdot f'[u_j(n+1)] W_{ji}(n+1). \quad (10)$$

$$\delta_i(N) = -[T_i - Y_i(N)]. \quad (11)$$

with $u_i(n)$ th input to the i^{th} neuron in n^{th} layer, L_{n+1} , the number of neurons in the $(n+1)^{\text{th}}$ layer, $f'(\cdot)$, a derivative of the sigmoid activation function over the input to the j^{th} neuron in $(n+1)^{\text{th}}$ layer. It is important, however, to remember that the training patterns must cover the entire range of input combinations for which the network will be required to perform accurate process emulation.

Since the input and output, variables of the ANN have different ranges, the feeding of the original data to the network leads to a convergence problem. In addition, the normalization of the inputs and outputs of the neurons network over an interval of [0-1] was done, to avoid a saturation effect of the sigmoid function.

3. THEORETICAL ANALYSIS

3.1. DETERMINATION OF CORONA ONSET VOLTAGES

Theoretical models to determine corona onset voltages (V_s) in strongly inhomogeneous fields (tip-plane configuration) have been proposed by several authors. Nitta's [22] model is based on the streamer criterion, and it is expressed in the following manner:

$$V_s = \left(\frac{E}{P} \right)_{\text{lim}} \cdot u.P.d \cdot \left(1 + \frac{C}{\sqrt{P.r_p}} \right). \quad (12)$$

E is the electric field, P is the gas pressure, u is the field utilization factor; r_p is the tip radius and d is the inter-electrode distance.

The constant C in equation (12) can be determined by the following equation:

$$C = \sqrt{\frac{4K}{\beta_m \left(\frac{E}{P}\right)_{\text{lim}}}}. \quad (13)$$

With K is the streamer criterion constant and β_m comes from the approximation of the ionization coefficient α of the mixture:

$$\alpha' = \beta_m \left[\left(\frac{E}{P}\right) - \left(\frac{E}{P}\right)_{\text{lim}} \right]. \quad (14)$$

Determination of $\left(\frac{E}{P}\right)_{\text{lim}}$

is defined by

$$\alpha' \left[\left(\frac{E}{P}\right)_{\text{lim}} \right] = 0. \quad (15)$$

The latter relation shows the value of the reduced field for which the equilibrium between ionization and attachment is realized. For $(E/P) > (E/P)_{\text{lim}}$, ionization becomes predominant and streamer phenomena occur in the gap, whereas for $(E/P) < (E/P)_{\text{lim}}$, there is no possibility to start a streamer.

Malik and Qureshi [23] calculated $(E/P)_{\text{lim}}$ for SF₆-N₂ mixtures making the assumption that:

$$\left(\frac{\alpha'}{P}\right)_{\text{lim}} = z \left(\frac{\alpha'}{P}\right)_{\text{SF}_6} + (1-z) \left(\frac{\alpha'}{P}\right)_{\text{N}_2}, \quad (16)$$

with z = ratio of SF₆.

However, since nitrogen and SF₆ do not interact with electrons of the same range of energy, this assumption is not rigorously exact. Kline and al. [24,25] have shown that there's good agreement between experimental results and those calculated using the empirical expression:

$$\left(\frac{E}{N}\right)_{\text{lim}} = \left(\frac{E}{N}\right)_{\text{SF}_6} \cdot (\% \text{SF}_6)^{0.18}. \quad (17)$$

3.2. EXPERIMENTALLY DEDUCED MOBILITIES

In a highly inhomogeneous configuration such as the point plane geometry, the theoretical determination of the mobility from the value of the mean electrical current was carried out using the following expression:

$$I = A \left(\frac{\mu \cdot \varepsilon}{d}\right) (V - V_0)^2, \quad (18)$$

where, ε is the dielectric constant of the gas, d is the point-plane distance. A is a constant, which, depends only on the geometry chosen.

To calculate the mobility in the point plane geometry, a simple geometric approximation is used instead of the real needle plane configuration.

R. Sigmond [26], considered the Warburg distribution on the plane electrode and obtained the unipolar saturation formula:

$$I_s = 2 \frac{\mu \varepsilon}{d} V^2. \quad (19)$$

Using Blanc's law [27], the mobility of gas mixture can be expressed by:

$$\frac{1}{\mu_i(\text{mixture})} = \frac{x_1}{\mu_1} + \frac{x_2}{\mu_2}, \quad (20)$$

where μ_1 and μ_2 are the mobility of the ions in the pure gases, x_1 and x_2 are respectively the mole fraction of the gas 1 and 2 in the mixture.

$$x_1 = \frac{N_1}{N_1 + N_2} \quad \text{and} \quad x_2 = \frac{N_2}{N_1 + N_2} = 1 - x_1. \quad (21)$$

3.3. DETERMINATION OF THE GAS TEMPERATURE

For a gas such as SF₆, where most of the constituents are diatoms, the total energy of any given molecule also includes the energy corresponding to the vibrational and rotational energy of the two atoms with respect to one another.

The vibrational temperature is related to the temperature of the vibrationally excited species, whereas the rotational temperature corresponds to the temperature of the neutrals [29,30]. At high-pressure collision between neutrals and the excited molecules are more effective and the rotational temperature tends to equilibrate with the kinetic temperature of the heavy species. Because of this, the rotational temperature (T_r) measured at high pressure is used to give the kinetic gas temperature [31].

In the present study, the spectra obtained from the light emission of SF₆-N₂ mixture were recorded with different values of pressure, voltage, and current together with the variation of the position of the tip electrode. The emission of N₂ is very dominant for different gas concentrations and the second positive system 2S⁺ is the most important. The convolution method [29-31] can be used to determine the discharge temperature by comparing the simulated spectrum obtained by the latter method and the experimental spectrum. The temperatures are determined by minimising the surface delimited between the two spectra.

This technique can be used as a spectroscopic thermometer.

4. EXPERIMENTAL DATA

Using the experimental setup shown previously [31] the measurements of the ionic mobility, the rotational temperatures, and the onset voltages were obtained using a tip-to-plane configuration.

The measurements of the current-voltage curves were done for different gas pressures ($I = f(V)$) and the mobility is determined from the slopes of ($\sqrt{I} = f(V)$) curves using R.S. Sigmond model [26].

Rotational temperatures of SF₆-N₂ gas mixture are spectroscopically measured over a pressure range of 2-14 bars. The spectra obtained from the light emission of the corona discharge were recorded with different values of pressure, voltage, and current together with the variation of the position of the tip electrode.

The measurements of the onset corona discharge voltages in SF₆-N₂ gas mixtures at higher pressure ranging from 2 to 14 bars and with different percentages of SF₆. The onset voltages were determined from the measurements of the current-voltage curves in both negative and positive polarities, with tip radii of a few micro-meters and the gap between the electrodes is lower than 10 mm.

5. RESULTS AND DISCUSSION

As an alternative to empirical prediction models, Artificial Neural Networks can be used to predict gas mixture parameters. The main feature of neural networks is the establishment of complex relationships between data through a learning process, with no need to previously propose any model to correlate the desired variables. The basic procedure is to use a database of measurements to train an ANN structure and then evaluate the predictive capacity of the built model on previously unseen data. As shown in Fig. 3 and 4, the best training performance of the neural network is obtained at epoch 213 ($1,0499 \cdot 10^{-11}$). The average relative error on predicted onset voltage is found to be less than 5% for our neuron network model.

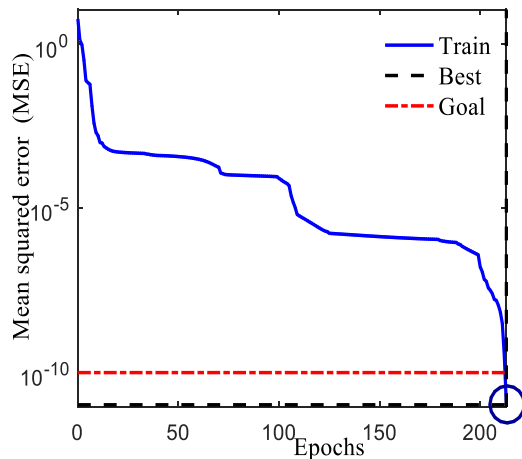


Fig. 3 – Best training performance of a neural network of onset voltage ($1,0499 \cdot 10^{-11}$ at epoch 213).

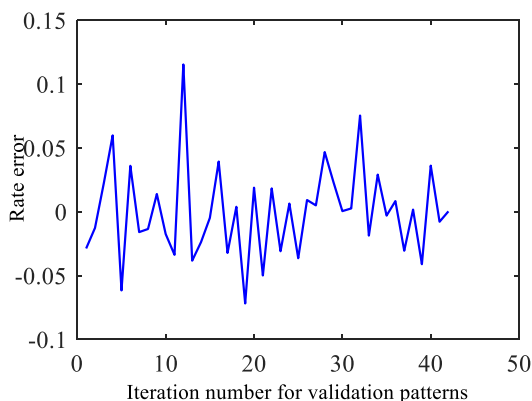


Fig. 4 – Average relative error with respect to iteration number of predicted onset breakdown voltage.

Figure 5 shows the experimental and predicted values of onset voltage with different amounts of SF₆ in the mixture as a function of the gas pressure for negative polarity. The values of corona inception voltages (V_s) increase linearly with pressure (P) and tend towards saturation at high values of pressure for both mixtures 100 % of SF₆ and 10 % SF₆ - 90 % N₂ [32,33]. As can be seen in figure 5, there is a total

concordance between the predicted and measured values of the onset voltages in pure SF₆ and in 10% SF₆ – 90 % N₂.

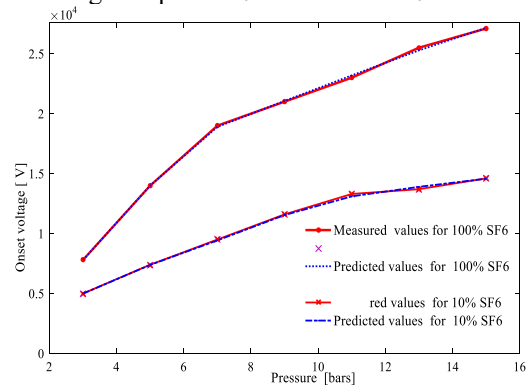


Fig. 5 – The variation of the onset voltage with the gas pressure for 10%SF₆-90%N₂ and pure SF₆ for a negative polarity.

For the prediction of ionic mobilities, Figs. 6-7 detail the mean square error and the average relative error obtained during the training procedure. The performance of ANN's training is shown in figure 6, where the convergence of the Levenberg-Marquardt algorithm is obtained at iteration 174 ($3,2726 \cdot 10^{-11}$): The average relative error on predicted mobilities is found to be less than 5% as can be seen in Fig. 7.

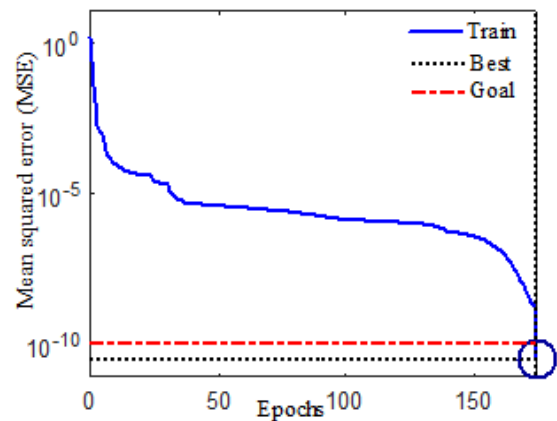


Fig. 6 – Best training performance of a neural network of ionic mobility ($3,2726 \cdot 10^{-11}$ at epoch 174).

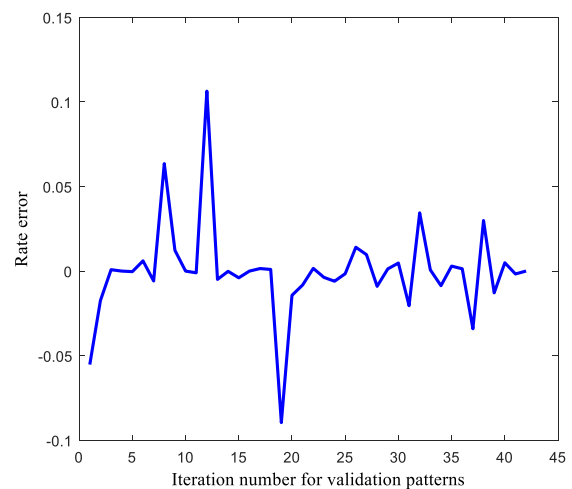


Fig. 7 – Average relative error with respect to iteration number of predicted ionic mobilities.

The curves of ANN's predicted values of ionic mobilities and the curves of determined values are shown in Fig. 8. The results clearly indicate a good agreement between the curves.

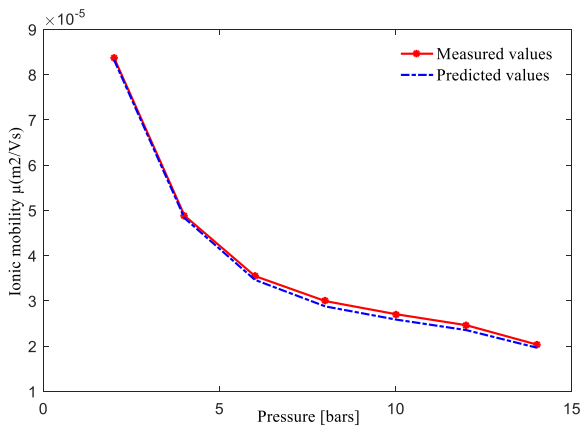


Fig. 8 – Measured and predicted ionic mobility, versus the gas pressure using ANN for 10 % SF₆-90 % N₂ in negative polarity.

The best training performance of the neural network of temperature is achieved at epoch 1000 ($2,2448.10^{-10}$), Fig. 9.

The relative error during the testing phase is under 4 % which is a very good measure to state the efficiency of the network architecture (figure 10).

The rotational temperature of SF₆-N₂ gas mixture was measured over a pressure range of 2-14 bars, as can be observed in figure 11, the predicted temperatures using the proposed ANN model are very consistent with the measured values.

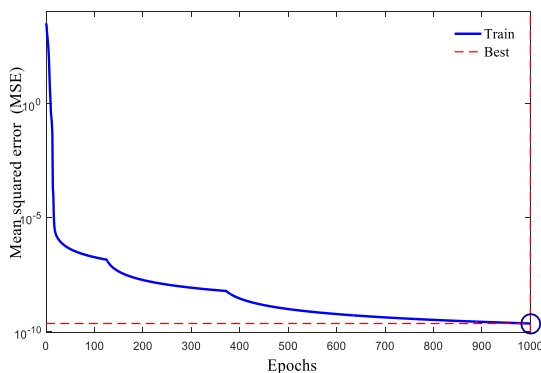


Fig. 9 – Best training performance of a neural network of temperature ($2,2448.10^{-10}$ at epoch 1000).

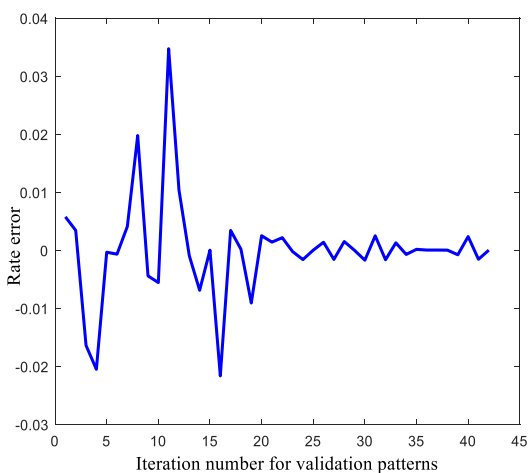


Fig. 10 – Average relative error with respect to iteration number of predicted rotational temperature.

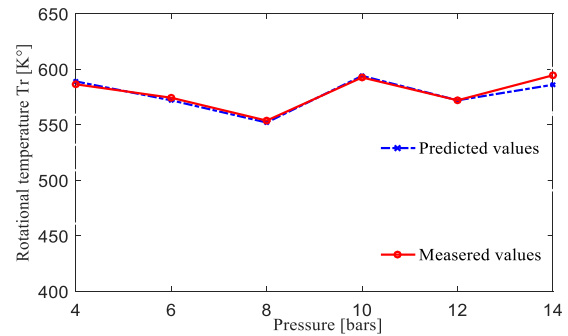


Fig. 11 – Measured and predicted rotational temperature, versus the gas pressure using ANN for 10 % SF₆ in negative polarity.

As shown in Fig.11, the variation of the temperature with the pressure with the value of the corona discharge current equals 5 μ A. It can be noticed that the effect of pressure is less important on the discharge temperature in mixture gas with an amount of 10 % of SF₆.

6. CONCLUSION

The application of neuron networks has become an important tool for estimating the variation of several parameters in insulators used in electrical systems [24-26], as in the present work the ANN can be very useful for the prediction of onset voltage, ion mobility and rotational temperature in SF₆-N₂ gas mixture, in the absence of mathematical models which give a precise prediction.

The prediction of these parameters using the proposed ANN is found to be in good agreement with the experimental values. The errors are always less than $\pm 6\%$ for training and testing. This technique can be a very useful prediction modeling tool for high voltage equipment.

For the same onset voltage, a mixture with 10% of SF₆ must work at approximately twice the pressure of pure SF₆. The variation of the mobility at elevated pressures is inversely proportional to the gas density. The mobility decreases with the increase of the amount of SF₆ in the gas mixture. In the present conditions, the effect of pressure on the temperature of the gas is not very important.

The comparison of the predicted results obtained by neural networks with those measured shows a good agreement for low SF₆ concentrations of 10 % SF₆ in mixtures, the difference is clearly observed.

Received on 12 July 2021.

REFERENCES

1. L. G. Christophorou, J.K. Olthof, R.J. Vanbrunt, *Sulfur Hexafluoride, and the Electric Power Industry*, IEEE Elec. Insul. Mag. **13**, 5, pp. 20-24 (1997).
2. L. Xingwen, H. Zhao, A. Bruce Murphy, *SF₆-N₂ alternative gases for application in gas-insulated switchgear*, J. Phys. D: Appl. Phys. **51**, 15, pp.153001-153025 (2018).
3. C.M. Franck, A. Chachereau, J. Pachin, *SF₆-free gas-insulated switchgear: current status and future trends*, IEEE, Electrical Insulation Magazine, **37**, 1, pp.1-23 (2021).
4. C. Breidenich, D. Magraw, J.W. Rubin, *The Kyoto Protocol to the United Nations Framework Convention on Climate Change*, American Journal of International Law, **92**, 2, pp. 315-331 (1998).
5. P. Forster, V. Ramaswamy, P. Artaxo, *et al.*, *Changes in Atmospheric Constituents and in Radiative Forcing*, Climate Change, The Physical Science Basis – Contribution of Working (2007).
6. Y. Kieffel, T. Irwin, P. Ponchon, J. Owens, *Green gas to replace SF₆ in electrical grids*, IEEE Power Energy Mag., **14**, pp.32-39 (2016).
7. European Union, Regulation (EU) No 517/2014 of the European

- Parliament and of the council of 16 April 2014 on, *fluorinated greenhouse gases and repealing Regulation (EC), N° 842/2006*, Official Journal of the European Union (2014).
8. G. Mauthe, L. Niemeyer, B.M. Pryor, R. Probst, H. Bräutigam, P.A. O'Connell, K. Pettersson, H.D. Morrison, J. Poblitzki, D. Koenig, *Task Force 01 of Working Group 23.10, SF₆ and the Global Atmosphere*, *Electra*, **164**, pp. 121–131 (1996).
 9. L. Niemeyer, F.Y. Chu, *SF₆ and the atmosphere*, *IEEE Trans. Electr. Insul.*, **27**, 1, pp. 184–187(1992).
 10. E. Kuffel, W.S. Zaengl, J. Kuffel, *High voltage engineering fundamentals*, Second edition, pp. 298-290 (2000).
 11. Y. P. Raizer, *Gas Discharge Physics*, Abridged translation of original Russian edition, *Fizika gazovogo razryada-* Moscovo, Nauka, Moscow, pp. 37-47 (1987).
 12. G.W. Irwin, K. Warwick, K. Hunt, *Neural network applications in control*, Pub. by the Institution of Electrical Engineers, London, United Kingdom, pp. 91-110 (1995).
 13. S. Haykin, *Neural Networks: a Comprehensive Foundation*, Upper Saddle River, N.J., Prentice Hall (1999).
 14. S.S. Tezcan, M.S. Dincer, H.R. Hiziroglu, *Calculation of Breakdown Voltages in Ar + SF₆ Using an Artificial Neural Network*, 2005 Annual Report Conference on Electrical Insulation and Dielectric Phenomena (2005).
 15. S.S. Tezcan, M.S. Dincer, H.R. *Prediction of breakdown voltages in N₂+SF₆ gas mixtures*, 2006 Annual Report Conference on Electrical Insulation and Dielectric Phenomena (2006).
 16. B. Monchusi, S. Letlotla, H. Ilgner, J. McGill, *Modeling of Breakdown Voltage by Artificial Neural Network*, 4th Robotics and Mechatronics Conference of South Africa (Robmech 2011) 23-25 November 2011, CSIR Pretoria South Africa (2011).
 17. K. Hornik, M. Stinchcombe, H. White, *Multilayer feed forward networks are universal approximations*, *Neural Networks*, **2**, 5, pp. 359-366 (1989).
 18. V. Kůrková, *Kolmogorov's theorem and multilayer neural networks*, *Neural Networks*, **5**, 3, pp. 501-506 (1992).
 19. Z. Wang, Y. Liu, P.J. Griffin, *A combined ANN and expert system tool for transformer fault diagnosis*. *IEEE Trans. Power Deliv.* **13**, pp.1224-1229 (2000).
 20. B.G. Kermania, S.S. Schiffman, H. Troy Naglea, *Performance of the Levenberg–Marquardt neural network training method in electronic nose applications*, *Sensors and Actuators B: Chemical*, **110**, 1, pp. 13-22 (2005).
 21. F.H. Pereira, F.E. Bezerra, S. Junior, J. Santos, and all, *Nonlinear Autoregressive Neural Network Models for Prediction of Transformer Oil-Dissolved Gas Concentrations*, *Energies*, **11**, 7, pp. 1-12 (2018).
 22. T. Nitta, Y. Shibuya, *Electrical breakdown of long gaps in sulfur hexafluoride*, *IEEE, Trans on Power Apparatus and Systems*, **90**, 3, pp.1065-1071 (1971).
 23. N.H. Malik, A.H. Qureshi, *Calculation of discharge inception voltages in SF₆-N₂ mixtures*, *IEEE, Trans. Elect. Insul.*, **EI-14**, 2, pp. 70-76 (1979).
 24. L.E. Kline, D.K. Davies, C.L. Chen, P.J. Chantry, *Dielectric Properties for SF₆ and SF₆ mixtures predicted from basic data*, *J. Appl. Phys.* **50**, 11, pp. 6789-6796 (1979).
 25. X. Li, H. Zhao, S. Jia, *Dielectric breakdown properties of SF₆-N₂ mixtures in the temperature range 300–3000 K*, *Journal of Physics D: Applied Physics*, **45**, 44, pp. 445202-445208 (2012).
 26. R.S. Sigmond, *Simple approximate treatment of unipolar space-charge-dominated coronas: The Warburg law and saturation current*, *J. Appl. Phys.* **53**, 2 (1982).
 27. E.W. McDaniel, E.A. Mason, *The mobility and diffusion of ions in gases*, 1973, by John Wiley & Sons, Inc. N.Y. N°2 (1979).
 28. G. Hinojosa and J. Urquijo, *Test of Blanc's law for negative ion mobility in mixtures of SF₆ with N₂, O₂ and air*, *J. Phys D: Appl. Phys.* **36**, pp. 2510-2514 (2003).
 29. A. Chelouah, E. Marode, G. Hartmann, S. Achat, *A new method for temperature evaluation in a nitrogen discharge*, *J. Phys. D: Appl. Phys.*, **27**, pp. 940-945 (1994).
 30. H. Champain, G. Hartmann, M. Lalmas, A. Goldman, *Spectroscopic study of high-pressure dc corona discharges in SF₆*, 11th Int. Con. of gas discharge and their applications, Tokyo, pp.152-155(1995).
 31. A. Lemzadmi, N. Bonifaci1, A. Denat, M. Nemamcha, *Light emission from corona discharge in SF₆ and SF₆/N₂ gas mixtures at high pressure*, *European. Physical. Journal. Appl. Phys.* **33**, pp. 213–219 (2006).
 32. A. Boudefel, A. Lemzadmi, A.Guerroui, A. Babouri, *Corona discharge in sulfur hexafluoride-nitrogen gas mixture*, *Rev. Roum. Sci. Techn. – Électrotechn. et Énerg.*, **60**, 2, pp. 153–161 (2015).
 33. A. Lemzadmi, A. Guerroui, A. Denat, *Onset corona discharge voltages in SF₆-N₂ gas mixtures at higher gas pressures*, 4th International Conference on Power Engineering, Energy and Electrical Drives (POWERENG), Istanbul Turkey, pp. 167-170 (2013).